



OPEN Resting state EEG reveals no reliable biomarkers of tinnitus laterality

Su Jin Kim¹, Seung-Ho Shin², Sung Wan Byun² & Ho Yun Lee^{2,3}✉

This study assessed whether resting-state quantitative EEG (qEEG) can differentiate tinnitus laterality under rigorous multiple-comparison control and nested, cross-validated machine learning (ML). We analyzed 210 pre-specified qEEG features—spectral power ($n = 95$), functional connectivity ($n = 80$), and hemispheric asymmetry indices ($n = 35$)—in 110 patients with chronic tinnitus (bilateral = 58, left = 27, right = 16, non-lateralized = 9). Group differences were tested with Kruskal–Wallis tests and Benjamini–Hochberg false discovery rate (FDR) correction ($q < 0.05$), followed by exploratory pairwise Mann–Whitney U tests and ANCOVA controlling for left-ear pure-tone average (PTA_L). No feature survived FDR in the four-group comparison. Although 48 features showed uncorrected $p < 0.05$ in at least one pairwise contrast, none remained significant after FDR. In the left–right contrast, effect sizes were small and post hoc power was low ($< 30\%$). ANCOVA indicated that most apparent differences were attributable to hearing asymmetry: after adjustment, no features survived FDR, covariate effects were small (median partial $\eta^2 \approx 0.01$), and results were unchanged after adjusting for interaural PTA asymmetry or mean PTA. Power modeling indicated that approximately 335 participants per group would be required to detect effects of $d = 0.23$ with 80% power. Nested ML models (random forest, SVM, logistic regression) performed at chance in four-class classification and near-chance in binary contrasts (balanced accuracy 57–63%; ROC AUC ≈ 0.56), mirroring weak univariate effects. Overall, resting-state scalp qEEG showed no robust cortical biomarkers of tinnitus laterality after multiple-comparison correction and adjustment for hearing thresholds; larger, balanced cohorts will be essential for future biomarker discovery.

Tinnitus, the phantom perception of sound without external acoustic stimulation, affects a substantial proportion of adults. A recent global meta-analysis estimated the pooled prevalence of any tinnitus at 14.4% and severe tinnitus at 2.3%, with considerable variation across studies (4.1%–37.2%) depending on assessment methods¹. The annual incidence of tinnitus was estimated at approximately 1% (1164 per 100,000 person-years)¹.

While tinnitus is frequently triggered by hearing loss from aging or noise exposure, it can also arise from head and neck trauma, ototoxic medications, or other medical conditions. Increasing evidence points to central mechanisms—such as elevated spontaneous firing and aberrant neural synchrony across auditory and non-auditory brain regions—as key contributors to tinnitus pathophysiology^{2,3}. Despite advances in understanding these mechanisms, tinnitus remains challenging to treat, partly due to its heterogeneous clinical presentations.

The laterality of tinnitus perception—whether localized to the left ear, right ear, both ears, or diffusely within the head—constitutes a fundamental clinical distinction that may reflect different underlying neural processes. Recent findings suggest that non-lateralized tinnitus, observed in approximately 10% of cases, is more common in older individuals with symmetrical high-frequency hearing loss and may represent an early, pre-habituational stage of tinnitus rather than a distinct subtype⁴. In contrast, lateralized tinnitus has been linked to prediction-error mechanisms within the auditory cortex, where a mismatch between expected and actual auditory input may recruit persistent top-down attentional systems that reinforce abnormal neural synchrony⁵. However, the neurophysiological underpinnings of tinnitus laterality remain incompletely understood, and peripheral hearing loss alone cannot fully account for the central features of this condition.

Neuroimaging and electrophysiological studies have identified abnormal neural activity associated with tinnitus, particularly in auditory cortical regions. A magnetoencephalography (MEG) study reported that tinnitus is associated with abnormal spontaneous brain activity, specifically reduced alpha and increased delta or gamma

¹Department of Otorhinolaryngology-Head and Neck Surgery, Kyung Hee University College of Medicine, Seoul, Korea. ²Department of Otorhinolaryngology-Head and Neck Surgery, Ewha Womans University School of Medicine, Seoul, Korea. ³Department of Otorhinolaryngology-Head and Neck Surgery, Ewha Womans University School of Medicine, Seoul, Republic of Korea. ✉email: hoyun1004@gmail.com

power in temporal regions⁶. This pattern likely reflects an imbalance between diminished cortical inhibition and enhanced excitatory processing, correlating with tinnitus-related distress⁶. Moreover, chronic tinnitus patients exhibit not only reduced alpha-band activity but also decreased moment-to-moment variability of auditory alpha oscillations—especially in the lower alpha range (8–10 Hz)—which may reflect impaired adaptive capacity of the auditory cortex and potentially serve as a neuroplasticity-related marker of persistent tinnitus⁷. Notably, oscillatory abnormalities in lateralized tinnitus are more pronounced in the contralateral hemisphere to the perceived tinnitus, suggesting a direct correspondence between tinnitus laterality and asymmetrical auditory cortical activity with intensity-dependent gamma oscillations reported in the contralateral auditory cortex^{7,8}.

Beyond localized spectral power changes, tinnitus appears to involve altered functional connectivity within and between brain networks. This includes disrupted interactions among the default mode, salience, and central executive networks—collectively described as the triple network model—which not only mediate tinnitus perception and distress but also account for its embodiment into self-identity and associated cognitive dysfunction, highlighting the need for individualized, network-targeted therapeutic approaches⁹. It remains unclear whether these connectivity patterns vary depending on tinnitus laterality. As tinnitus varies widely in clinical presentation, more personalized and targeted treatment strategies are essential. Developing reliable biological markers for meaningful patient stratification may be a key step toward this goal¹⁰. However, markers that can differentiate subtypes, especially by laterality, remain unavailable in everyday clinical practice.

Recently, machine learning methods have been used in analyzing and uncovering the neurophysiological signatures of tinnitus. For example, resting-state EEG connectivity features—such as phase-locking value (PLV) and Pearson correlation coefficient (PCC)—can reliably classify tinnitus laterality, achieving over 99% accuracy in prediction models¹¹. However, these findings were based on a relatively small and highly selected sample ($N=50$) without including head-centered tinnitus. That study used a simplified three-group classification (left, right, bilateral), which may limit how well the findings apply to the broader clinical population. In addition, the emphasis was mainly placed on achieving high classification accuracy, with less attention given to understanding the underlying brain mechanisms or explaining how the predictive features relate to tinnitus physiology.

Exploring how neurophysiological patterns vary with tinnitus laterality could shed light on its underlying mechanisms and help guide more personalized treatment approaches. At present, neuromodulatory therapies are often delivered uniformly without considering the specific side or distribution of the tinnitus percept—a practice that may partly account for their inconsistent clinical results. Adjusting stimulation parameters to match each patient's brain activity profile could improve therapeutic effectiveness.

This study analyzed qEEG data from 110 tinnitus patients to investigate neurophysiological differences associated with tinnitus laterality. We employed a comprehensive approach examining power spectra, interhemispheric coherence, and phase-locking values across multiple frequency bands, complemented by machine learning classification techniques. We aimed to identify characteristic EEG patterns and functional connectivity differences that could inform the development of targeted neuromodulatory treatments and advance our understanding of the neural mechanisms underlying different tinnitus laterality presentations.

While it is widely accepted that tinnitus is a central nervous system disorder, the precise relationship between peripheral auditory deficits and the emergence of specific neurophysiological signatures remains incompletely understood. A critical unresolved question is how a peripheral condition, such as asymmetrical hearing loss, translates into distinct patterns of cortical dysfunction that govern the perceptual laterality of tinnitus. This study, therefore, was designed to bridge this explanatory gap. By leveraging qEEG and machine learning, we aimed not only to identify the characteristic neurophysiological profiles for each laterality subtype but also to elucidate how these central patterns are associated with peripheral hearing status. We hypothesized that asymmetrical hearing loss serves as a primary trigger, initiating distinct and measurable patterns of maladaptive cortical plasticity that define tinnitus laterality.

Results

Clinical characteristics by tinnitus laterality

Clinical characteristics are described in Table 1. Patients with right-sided tinnitus were significantly younger (mean age 45.3 ± 12.5 years) compared to other groups (bilateral: 55.5 ± 13.3 , left: 55.7 ± 13.1 , non-lateralized: 50.7 ± 8.5 years). The left-sided tinnitus group demonstrated the highest tinnitus awareness scores (8.70 ± 1.94), while the bilateral group reported the highest tinnitus loudness (7.53 ± 1.91) and annoyance (7.79 ± 2.42) ratings. Notably, left-sided tinnitus patients exhibited the lowest mean THI score (49.9 ± 23.9), whereas bilateral tinnitus patients showed the highest (54.4 ± 26.1).

Audiometric findings revealed significant differences in left ear hearing thresholds across groups ($p=0.006$), with the most pronounced differences between left and right tinnitus groups ($p=0.002$). Associated symptoms, including sleep disturbance, temporomandibular or neck pain, and headache, also showed differential distribution across laterality groups, with non-lateralized tinnitus demonstrating stronger associations with sleep disturbance ($p=0.011$) and neck pain ($p=0.036$).

Primary analysis: four-group qEEG comparison

Our primary, pre-specified analysis aimed to identify neurophysiological differences across the four tinnitus laterality groups. We conducted Kruskal–Wallis tests on all 210 qEEG features, followed by a rigorous false discovery rate (FDR) correction for multiple comparisons. This analysis revealed no statistically significant differences for any feature (all adjusted $p>0.05$). Although a small number of features showed uncorrected p -values below 0.05, a rate consistent with the expected number of false positives, none survived the FDR correction. The distribution of p -values from this primary analysis, illustrating the null finding, is shown in Fig. 1.

Characteristic	Bilateral (n = 58)	Left (n = 27)	Right (n = 16)	Non-lateralized (n = 9)	p value
Age, mean \pm SD	55.5 \pm 13.3	55.7 \pm 13.1	45.3 \pm 12.5	50.7 \pm 8.5	0.024*
Male, n (%)	32 (55.2)	16 (59.3)	10 (62.5)	3 (33.3)	0.342
Female, n (%)	26 (44.8)	11 (40.7)	6 (37.5)	6 (66.7)	0.342
Tinnitus duration, years, median (IQR)	3.2 (1.4–6.8)	2.9 (1.1–5.5)	2.1 (0.9–4.1)	2.5 (1.2–5.2)	0.137
THI score, mean \pm SD	54.4 \pm 26.1	49.9 \pm 23.9	52.8 \pm 24.2	51.3 \pm 22.1	0.872
VAS Awareness	8.34 \pm 1.86	8.70 \pm 1.94	7.88 \pm 2.03	8.44 \pm 1.67	0.419
VAS Annoyance	7.79 \pm 2.42	7.59 \pm 2.21	7.25 \pm 2.35	7.33 \pm 2.06	0.778
VAS Loudness	7.53 \pm 1.91	7.41 \pm 1.78	6.94 \pm 2.05	7.11 \pm 1.90	0.641
VAS Effect on life	7.22 \pm 2.54	6.89 \pm 2.34	6.56 \pm 2.22	7.00 \pm 2.18	0.716
PTA (Right)	24.3 \pm 17.2	18.7 \pm 12.4	27.9 \pm 19.5	21.6 \pm 14.8	0.195
PTA (Left)	23.8 \pm 16.4	32.6 \pm 18.7	17.2 \pm 13.1	22.2 \pm 15.6	0.006**
Subjective hyperacusis, n (%)	35 (60.3)	14 (51.9)	9 (56.3)	6 (66.7)	0.794
Sleep disturbance, n (%)	28 (48.3)	11 (40.7)	5 (31.3)	8 (88.9)	0.011*
Headache, n (%)	19 (32.8)	10 (37.0)	4 (25.0)	5 (55.6)	0.382
Pain, n (%)	22 (37.9)	9 (33.3)	5 (31.3)	7 (77.8)	0.036*
Dizziness, n (%)	17 (29.3)	8 (29.6)	3 (18.8)	4 (44.4)	0.479
Aural fullness, n (%)	26 (44.8)	13 (48.1)	6 (37.5)	5 (55.6)	0.784

Table 1. Demographic and audiological characteristics by tinnitus laterality. * $p < 0.05$, ** $p < 0.01$ Kruskal–Wallis test (continuous variables) or chi-square test (categorical variables). THI, tinnitus handicap inventory; VAS, visual analog scale; PTA, pure tone average; IQR, interquartile range.

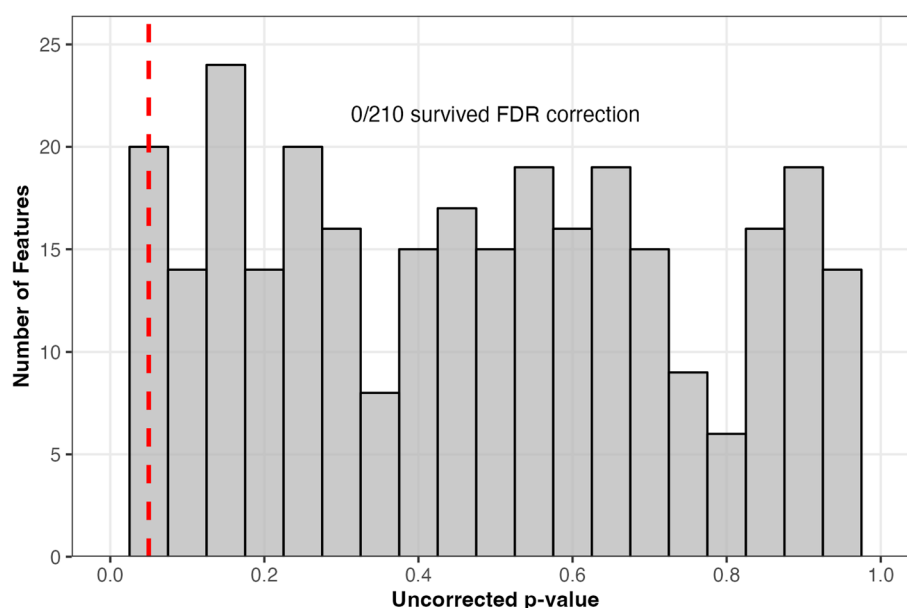


Fig. 1. P-value Distributions from primary four-group comparison. The distribution of uncorrected p-values from the primary Kruskal–Wallis tests comparing all four laterality groups across 210 qEEG features. The relatively uniform distribution is consistent with an overall null finding, as no features survived false discovery rate (FDR) correction.

Exploratory post-hoc analysis

After multiple comparison correction using the Benjamini–Hochberg method, no features remained significant at $FDR < 0.05$. Therefore, we conducted exploratory analyses using uncorrected p-values, which revealed 48 features with $p < 0.05$ in at least one contrast (Table 2). Across contrasts, the distributions of absolute effect sizes were small (median |Cohen's d | \approx 0.19–0.23; Fig. 2).

Right-sided vs. bilateral tinnitus showed the most pronounced differences, accounting for 30 of the 48 significant features. In this comparison, theta-band power at multiple cortical sites was consistently elevated in the bilateral group, including central (Cz theta, $p = 0.002$; C3 theta, $p = 0.007$; C4 theta, $p = 0.014$) and posterior regions (P4 theta, $p = 0.008$; Pz theta, $p = 0.011$; P3 theta, $p = 0.034$). The effect sizes for these theta differences were moderate ($|d| = 0.53$ – 0.67).

Feature	Left vs. Right	Left vs. Bilateral	Right vs. Bilateral	Unilateral vs. Bilateral	Max d
Cz theta	0.028	–	0.002	0.012	0.64
FP1 theta	0.028	–	0.005	0.031	0.60
P4 theta	0.020	–	0.008	0.027	0.56
PTA L	0.002	0.007	–	–	1.04
T3 theta	0.019	–	0.006	–	0.78
C4 gamma	0.013	0.017	–	–	0.78
F4 theta	0.028	–	0.018	–	0.67
C3 theta	–	–	0.007	0.040	0.67
FP2 theta	0.026	–	0.013	–	0.66
Cz gamma	0.041	0.024	–	–	0.66
F7 theta	–	–	0.008	0.034	0.66
T5 delta	0.016	–	0.049	–	0.65
T3 alpha	0.026	–	0.010	–	0.64
F3 theta	–	–	0.011	0.027	0.62
T4 gamma	0.014	–	0.028	–	0.58
F7 delta	–	–	0.025	0.026	0.58
Fz delta	–	–	0.015	0.026	0.56
Fz theta	–	–	0.033	0.042	0.55
T6 theta	–	–	0.007	0.017	0.54
Pz theta	–	–	0.011	0.018	0.53
F3 gamma	0.046	0.041	–	–	0.52
P4 alpha	0.041	–	0.012	–	0.52
FP1 alpha	0.046	–	0.028	–	0.51
Cz alpha	0.049	–	0.017	–	0.47
COH T5 T6 theta	–	–	0.024	0.011	0.35
O1 theta	0.023	–	–	–	0.71
C3 delta	–	–	0.033	–	0.68
Cz beta	–	0.020	–	–	0.64
PLV T3 T4 delta	0.036	–	–	–	0.63
F8 theta	–	–	0.028	–	0.59
T4 theta	–	–	0.029	–	0.58
A1 FP1 FP2 alpha	–	–	–	0.032	0.58
P4 delta	–	–	0.037	–	0.57
T4 alpha	0.046	–	–	–	0.56
Fz gamma	–	0.040	–	–	0.56
C4 theta	–	–	0.014	–	0.55
P3 theta	–	–	0.034	–	0.54
A1 T3 T4 delta	–	–	–	0.045	0.52
F7 alpha	–	–	0.031	–	0.51
F3 delta	–	–	0.034	–	0.51
P3 alpha	–	–	0.036	–	0.50
FP1 delta	–	–	0.036	–	0.49
C3 alpha	–	–	0.024	–	0.49
T6 alpha	–	–	0.041	–	0.48
Pz alpha	–	–	0.022	–	0.47
T6 delta	–	–	0.043	–	0.46
O2 theta	–	–	0.045	–	0.46
C4 alpha	–	–	0.039	–	0.43

Table 2. Features with uncorrected $p < 0.05$ in at least one pairwise comparison. Values are uncorrected p -values; ‘–’ indicates $p \geq 0.05$. Max|d| is the largest absolute Cohen’s d observed across the four contrasts. No feature survived FDR correction (all adjusted $p > 0.05$).

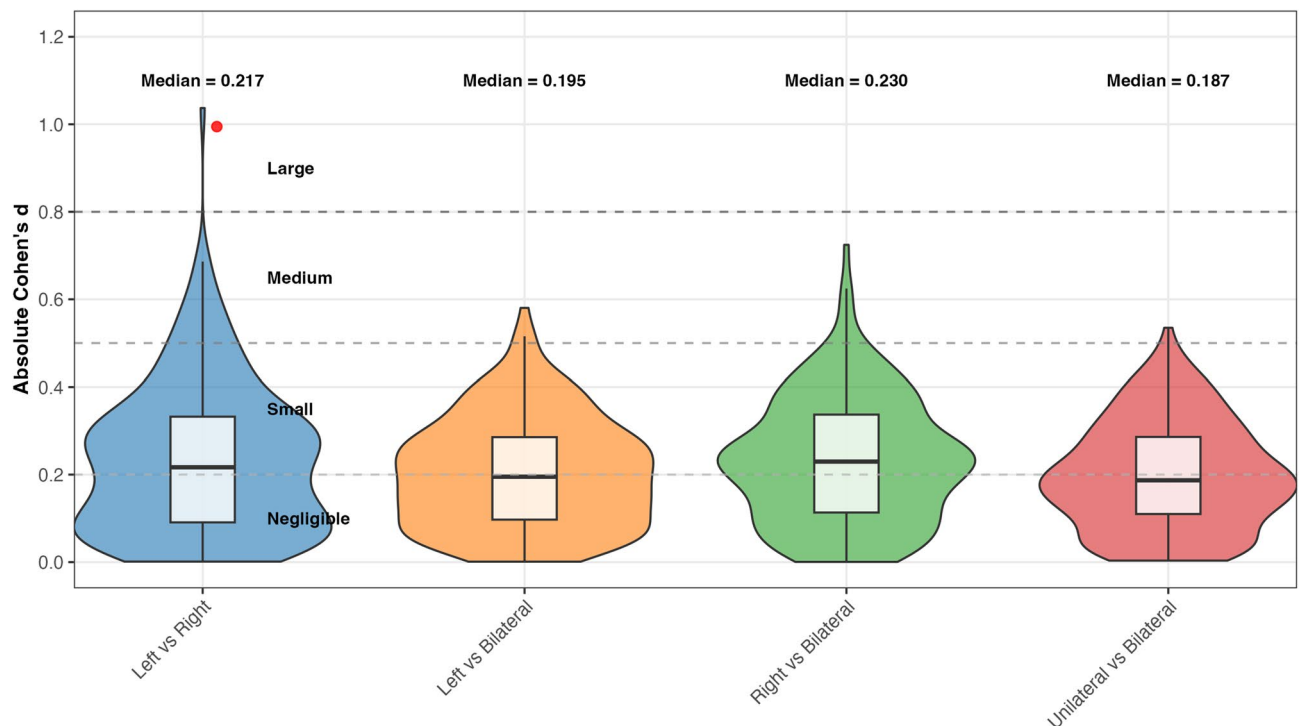


Fig. 2. Effect size distributions for all post-hoc pairwise comparisons. Violin plots show the distribution of absolute Cohen's d values, with box plots indicating median and interquartile ranges. Horizontal dashed lines mark conventional effect size boundaries. Numbers below each comparison indicate total features analyzed, while numbers above show median effect sizes. The predominance of small effects ($|d| < 0.5$) across all comparisons supports the absence of robust neurophysiological differences between laterality groups.

The left- vs. right-sided tinnitus comparison yielded 17 significant features, with generally small effect sizes (median $|d| \approx 0.22$; Fig. 2). Notable findings included differences in gamma power at central sites (C4 gamma, $p = 0.013$, $|d| = 0.78$; Cz gamma, $p = 0.041$, $|d| = 0.66$) and inter-hemispheric connectivity (PLV T3-T4 delta, $p = 0.036$, $|d| = 0.63$). PTA_L showed the largest effect size across all comparisons ($p = 0.002$, $|d| = 1.04$), indicating a strong association between hearing thresholds and tinnitus laterality.

The unilateral (combined left and right) versus bilateral comparison revealed 11 significant features. Similar to the right-bilateral comparison, theta power was generally higher in bilateral tinnitus at frontal and central sites (Fz theta, $p = 0.042$; C3 theta, $p = 0.040$), while inter-hemispheric connectivity measures showed mixed patterns (COH T5-T6 theta, $p = 0.011$, $|d| = 0.35$).

The left-sided vs. bilateral comparison showed the fewest differences, with only six significant features, all demonstrating small effect sizes. These included PTA_L ($p = 0.007$) and scattered gamma-band differences (Cz gamma, $p = 0.024$; F3 gamma, $p = 0.041$).

Overall, while these exploratory findings suggest potentially higher low-frequency power in bilateral tinnitus and some connectivity differences between unilateral and bilateral presentations, the lack of significance after correction for multiple comparisons and generally small effect sizes warrant cautious interpretation.

Power analysis

With our actual sample sizes and the small median effect sizes observed (Cohen's d ranging from 0.19 to 0.23), we achieved only minimal statistical power across all comparisons. Specifically, the power to detect differences ranged from 10.3% for the left-sided versus right-sided tinnitus comparison ($n = 27$ vs. 16) to 15.8% for the unilateral versus bilateral comparison ($n = 43$ vs. 58). These low power values indicate that our study had less than a 16% chance of detecting actual differences of the magnitude observed. Reaching the usual 80% statistical power would require far bigger cohorts than we have 335 patients per group for an effect size of 0.23 and up to about 450 per group for an effect size of 0.19.

ANCOVA results

To assess whether peripheral hearing influenced the observed qEEG differences, we ran permutation-based ANCOVA with left-ear pure-tone average (PTA_L) as a covariate. After adjustment, the number of uncorrected $p < 0.05$ features decreased markedly—for example, in the Left-vs-Bilateral comparison from 34 to 7—and no feature survived FDR correction in any comparison. Effect sizes were uniformly small (median partial $\eta^2 \approx 0.01$; ≈ 0.09 – 0.12 in Cohen's f), and PTA_L explained $> 10\%$ of variance in only 2/210 features. A sensitivity analysis using either interaural PTA asymmetry (PTA_L–PTA_R) or mean PTA as the covariate yielded the same results: counts of uncorrected findings varied slightly across comparisons, but no laterality effect met $FDR < 0.05$, and

covariate effects remained small (median partial $\eta^2 \approx 0.01$ for both). Taken together with the interaural hearing asymmetry aligned with tinnitus laterality in Table 1, these results indicate that hearing thresholds are a major contributor to the apparent group effects, whereas residual qEEG differences are exploratory.

As visualized in Fig. 3A as a subset of features changed significance status after covariate adjustment: 7 features newly gained significance (e.g., PLV T3–C3 delta, AI F3–F4 gamma), while six features lost significance (e.g., Coherence T4–C4 theta, P3 gamma power). Figure 3B further illustrates that features based on spectral power were disproportionately affected, with multiple power-related variables (e.g., T3 alpha power, O1 theta power) losing statistical significance. In contrast, connectivity features, including PLV and AI metrics, particularly in the gamma and delta bands, were more likely to gain significance after controlling for PTA. However, these trend-level findings did not survive FDR and should be interpreted as exploratory rather than evidence of effects independent of hearing.

Machine learning classification and feature importance

Machine learning approaches were employed to evaluate whether multivariate patterns of qEEG features could classify tinnitus laterality. After the failure of the four-group classification (performing at a 25% chance level), we conducted binary classifications for all post-hoc comparisons: left vs. right, left vs. bilateral, right vs. bilateral, and unilateral vs. bilateral. Three algorithms—Random Forest (RF), Support Vector Machine (SVM), and Logistic Regression (LR)—were evaluated using leave-one-out cross-validation for smaller samples ($n < 30$) or fivefold cross-validation for larger samples. All analyses faced substantial data reduction due to missing qEEG values, with complete-case availability ranging from 39.5% (17/43) for left-sided vs right-sided to 50.0% (37/74) for right-sided vs bilateral (Table 3).

For inference, we report nested cross-validation performance using balanced accuracy and ROC AUC (Fig. 4). Across contrasts, balanced accuracy was 57–63% and ROC AUC was approximately 0.56, i.e., near-chance, with unstable feature-importance rankings across folds.

For transparency, Table 3 reproduces the accuracy values from the original CV scheme (LOOCV for very small samples; fivefold otherwise). Because accuracy can be inflated under class imbalance, these values should be interpreted with caution; balanced accuracy and AUC (Fig. 4) provide the preferred summary of discriminative performance. Feature-importance profiles varied by fold and model, and no feature set showed consistent, replicable importance across resamples. Taken together with the null univariate results, these findings suggest that, in our dataset, resting-state scalp qEEG is unlikely to support reliable laterality classification.

Discussion

In this study, we aimed to identify neurophysiological markers of tinnitus laterality using 210 qEEG features. The four-group comparison yielded a clear null result—none of the features remained significant after FDR correction, despite thorough statistical testing. This suggests that tinnitus is highly heterogeneous and that any cortical differences linked to perceptual laterality are likely subtle or vary considerably between individuals¹². Exploratory post-hoc testing (uncorrected) identified 48 features with $p < 0.05$ across the four pairwise contrasts

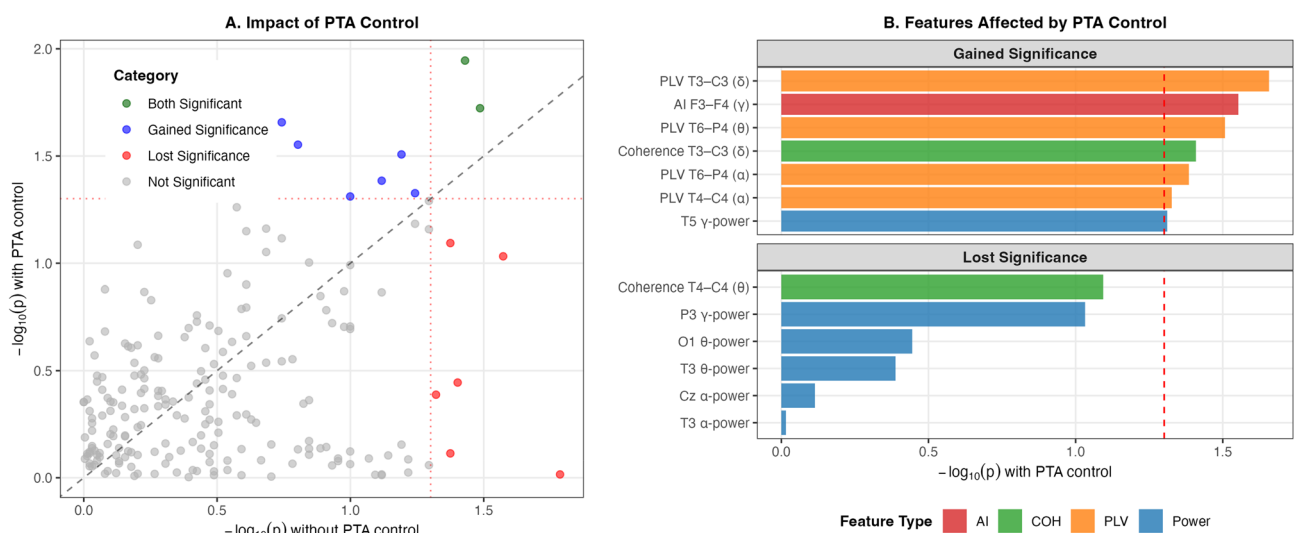


Fig. 3. Impact of hearing-threshold covariate control on feature significance. (A) Scatterplot of $-\log_{10}(p)$ values before (x-axis) and after (y-axis) controlling for left-ear pure-tone average (PTA_L) using permutation ANCOVA ($n = 110, 210$ features). Each point represents a qEEG feature, colored by significance status: green = significant in both models, blue = gained significance, red = lost significance, gray = not significant. Dotted lines indicate the uncorrected $p = 0.05$ threshold ($-\log_{10} \approx 1.30$), and the dashed diagonal represents the identity line. (B) Features that gained (top) or lost (bottom) significance after PTA_L adjustment, ranked by $-\log_{10}(p)$. Feature types are color-coded: red = AI, green = coherence, orange = PLV, blue = spectral power. The vertical dashed line marks the $p = 0.05$ threshold.

Comparison	Sample size	Model	Accuracy	AUC
Left vs. Right	17/43 (39.5%)	RF	62.8%	0.569
		SVM	55.8%	0.572
		LR	60.5%	0.648
Left vs. Bilateral	32/85 (37.6%)	RF	72.9%	0.750
		SVM	66.7%	0.469
		LR	55.3%	0.557
Right vs. Bilateral	37/74 (50.0%)	RF	77.7%	0.515
		SVM	78.4%	0.564
		LR	63.5%	0.467
Unilateral vs. Bilateral	42/101 (41.6%)	RF	61.9%	0.625
		SVM	56.4%	0.536
		LR	52.5%	0.539

Table 3. Machine Learning performance. RF; Random Forest, SVM; Support Vector Machine (SVM) radial-basis-function, LR; Logistic Regression Note: Accuracy/AUC are from the original LOOCV/fivefold scheme and may be affected by class imbalance; balanced accuracy and AUC from nested cross-validation are reported in Fig. 4

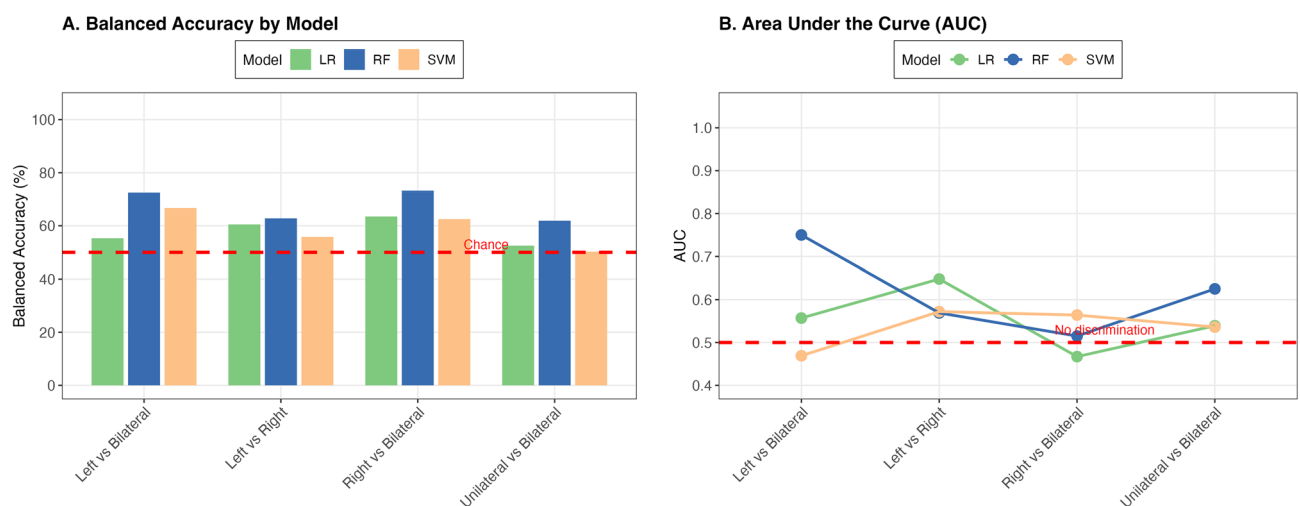


Fig. 4. Classification accuracy and discriminative performance of machine learning models across tinnitus laterality comparisons. **(A)** Balanced accuracy (%) for three classifiers—logistic regression (LR), random forest (RF), and support vector machine (SVM)—across four binary comparisons (Left vs Bilateral, Left vs Right, Right vs Bilateral, Unilateral vs Bilateral). Values are means across outer folds of the nested cross-validation; red dashed line = chance (0.50). **(B)** ROC AUC for the same models and comparisons; red dashed line = no discrimination (AUC = 0.50). Balanced accuracy mitigates effects of class imbalance. Across tasks, both metrics remained close to chance, indicating limited discriminative information in scalp qEEG for laterality.

(Table 2). Most detections arose from the right-sided vs. bilateral comparison, where theta-band power at central/posterior sites was consistently higher in the bilateral group (e.g., Cz theta $p = 0.002$, $|d| = 0.64$). The left-sided vs. right-sided comparison showed roughly half as many nominal effects, highlighted by central gamma power (C4 gamma $p = 0.013$, $|d| = 0.78$). The unilateral- vs. bilateral and left-sided vs. bilateral contrasts yielded progressively fewer findings (≈ 11 and 6, respectively). All results are exploratory; no feature survived FDR correction.

To assess the influence of hearing, we ran permutation ANCOVA with left-ear PTA (PTA_L) as a covariate and repeated the analysis using interaural PTA asymmetry (PTA_L–PTA_R) or mean PTA. Across specifications, most spectral-power differences attenuated, no laterality term met $FDR < 0.05$, and covariate effects were small (median partial $\eta^2 \approx 0.01$). Together with the interaural hearing asymmetry aligned with the tinnitus side (Table 1), these results indicate that hearing thresholds are a major contributor to the apparent group differences; any residual EEG patterns are small and exploratory.

A cautious interpretation is that peripheral asymmetry may account for local spectral-power differences (alpha/theta), whereas connectivity measures occasionally showed trend-level (uncorrected) differences after adjustment. These trends do not establish reorganization independent of hearing asymmetry and should be considered hypothesis-generating. Observations such as elevated theta power in bilateral tinnitus are consistent

with mechanistic frameworks (e.g., thalamocortical dysrhythmia), but our data do not provide corrected evidence for laterality-specific cortical markers; larger, preregistered cohorts with independent replication and complementary imaging will be required.

Although no features survived correction in our exploratory analyses, the bilateral tinnitus group exhibited elevated theta-band power, a pattern potentially reflecting thalamocortical dysrhythmia—a model positing that deafferentation leads to increased low-frequency activity and compensatory gamma activation¹³. This theory remains a cornerstone in understanding tinnitus pathophysiology and has been expanded upon in recent network-based models^{9,14}. In contrast, the unilateral tinnitus group showed enhanced interhemispheric connectivity, which may represent callosal compensation or rebalancing mechanisms following asymmetric input¹⁵.

These exploratory findings must be interpreted with caution, but they are conceptually consistent with broader frameworks of tinnitus pathophysiology that involve both localized excitability and distributed network disruption.

Our results have several important clinical implications. First, despite some models achieving greater than 70% classification accuracy in post-hoc ML analyses, the poor AUC values (0.51–0.75) and imbalanced sensitivity–specificity profiles indicate limited clinical utility of current qEEG-based models in predicting tinnitus laterality. For example, the SVM model in the unilateral vs. bilateral comparison showed 92% specificity but only 8.5% sensitivity, essentially defaulting to majority class predictions.

Second, scalp qEEG using conventional spectral and connectivity features—while valuable for hypothesis generation—appears insufficient for clinical stratification of tinnitus subtypes¹⁶. However, our findings suggest that gamma-band connectivity, especially in temporo-parietal regions, may serve as a central biomarker worth pursuing in future frameworks. Supporting this, a recent study applying wavelet-based frequency decomposition and microstate modeling identified distinct alterations in beta and gamma band dynamics—particularly in microstate duration and transition probabilities—that enabled near-perfect classification of tinnitus patients using deep neural networks, with up to 100% accuracy in the gamma band under eyes-open conditions¹⁷. These findings suggest that microstate-based temporal features, rather than traditional EEG measures alone, may offer more robust biomarkers for tinnitus. In turn, neuromodulatory treatments could be more effective if they target abnormal network connectivity—especially in the gamma band—rather than focusing only on localized cortical activity. EEG-guided or connectivity-informed interventions such as tACS or neurofeedback may thus offer personalized treatment options for lateralized tinnitus¹⁸.

This study has several critical limitations. The most significant is the statistical approach. Our progression from a failed primary four-group comparison to an exploratory post-hoc analysis of a specific subgroup substantially increases the risk of Type I error. The reported adjusted p-values in our post-hoc analysis do not account for the selection bias introduced by this sequential, data-driven strategy. Second, the study was limited by its constrained statistical power and severe sample size imbalance. The small sample sizes for the right-sided ($n = 16$) and non-lateralized ($n = 9$) groups were insufficient to detect anything but very large effects, which is a likely contributor to the null findings in our primary analysis. Third, the retrospective design of the study introduces potential biases. Our analysis was based on clinically collected data, which may introduce selection bias and variability in how measurements were obtained. In addition, the cross-sectional nature of the study limits our ability to draw causal inferences between the observed neurophysiological patterns and tinnitus laterality; we can only describe associations.

Finally, while qEEG offered valuable insights in this study, it also comes with important limitations. Because EEG primarily reflects cortical surface activity, its spatial resolution is relatively low, and it cannot directly capture signals from deeper brain structures such as the thalamus or amygdala—regions thought to be central to tinnitus pathophysiology. To overcome these constraints, future studies should adopt prospective designs with larger and more balanced samples, and consider incorporating multimodal imaging techniques to better map the complex neural networks involved in tinnitus laterality.

Conclusion

Despite analyzing 210 qEEG features in 110 patients with tinnitus, we found no statistically reliable markers of laterality after adjusting for multiple comparisons. The observed median effect size ($d = 0.217$) suggests that a sample size of approximately 335 participants per group would be necessary to achieve sufficient statistical power.

Methods

Study design and population

This study analyzed data from 110 patients who visited a tinnitus clinic within a tertiary university hospital between March 2020 and March 2025. All patients underwent comprehensive clinical assessment and 19-channel quantitative electroencephalography (qEEG) as part of their initial evaluation. Patients were categorized by tinnitus laterality into four groups: bilateral ($n = 58$), left ($n = 27$), right ($n = 16$), and non-lateralized ($n = 9$).

Ethics approval and consent to participate

All methods were carried out in accordance with relevant guidelines and regulations, including the Declaration of Helsinki. All experimental protocols were approved by the Ewha Womans University Mokdong Hospital Institutional Review Board (Seoul, Republic of Korea; approval No. EUMC 2025–02–011). Due to the retrospective nature of the study, the Ewha Womans University Mokdong Hospital Institutional Review Board waived the need of obtaining informed consent.

Clinical assessment

Standard clinical evaluation included detailed medical history and comprehensive audiological assessment. Tinnitus-related distress and characteristics were evaluated using the Tinnitus Handicap Inventory (THI) and visual analog scales (VAS, 0–10) measuring tinnitus awareness, annoyance, loudness, and effect on daily life. The audiometric assessment included pure-tone audiometry to calculate pure-tone averages at 0.5, 1, 2, and 4 kHz for each ear.

Psychological evaluation included the Hospital Anxiety and Depression Scale (HAD), Beck Depression Inventory (BDI), and Beck Anxiety Inventory (BAI). Additional clinical variables assessed included the Mini-Mental State Examination (MMSE), subjective hyperacusis, sleep quality, headache, neck pain, dizziness, and aural fullness. All measurements were obtained during the patient's initial clinic visit.

Quantitative EEG acquisition and processing

Resting-state EEG recordings were performed as part of the standard initial evaluation using a 19-channel MINDD scan system (Ybrain, Republic of Korea) with electrode placement according to the International 10–20 system. Data were acquired at a sampling rate of 500 Hz with electrode impedances maintained below five k Ω . Patients were instructed to sit comfortably with eyes closed in a sound-attenuated, electrically shielded room for 20 min. A trained technician continuously monitored the recordings for signs of drowsiness and provided verbal alerts if necessary to ensure a state of relaxed wakefulness. This acquisition protocol was consistent with our previous study investigating neural correlates of tinnitus-related cognitive changes¹⁸.

Raw EEG data underwent preprocessing, including band-pass filtering (0.5–70 Hz), notch filtering (60 Hz), and artifact rejection. Independent component analysis was applied to remove ocular, cardiac, and muscular artifacts. Preprocessed data were segmented into 2-s epochs, and epochs containing residual artifacts or sleep markers (e.g., vertex waves, K-complexes, sleep spindles) were manually rejected by a trained specialist blind to the patient's clinical information.

qEEG features extraction

Spectral features were extracted using MATLAB-based custom scripts integrated with EEGLAB. We systematically extracted a total of 210 qEEG features from the preprocessed data for each participant. These features comprised 95 spectral power features, which were derived from five distinct frequency bands (delta: 1–4 Hz, theta: 4–8 Hz, alpha: 8–13 Hz, beta: 13–30 Hz, gamma: 30–45 Hz) across all 19 electrodes. An additional 80 functional connectivity features were calculated for eight key electrode pairs (T3–T4, T5–T6, T3–F3, T4–F4, T3–C3, T4–C4, T5–P3, T6–P4) across the five frequency bands, using both the phase-locking value (PLV) and magnitude squared coherence (MSC). Finally, 35 hemispheric asymmetry indices were computed for seven homologous electrode pairs using the formula: $AI = \log(\text{right hemispheric power}) - \log(\text{left hemispheric power})$. Power spectral density values were log10-transformed to normalize distributions before statistical analysis. These features were then merged with clinical and audiological data for subsequent statistical analysis.

Statistical analysis

Our statistical analysis was conducted in a sequential, two-stage data-driven approach. In Stage 1 for Primary Analysis, we conducted Kruskal–Wallis tests to compare all four laterality groups across all 210 qEEG features as well as demographic and clinical characteristics. Chi-square analysis was performed for categorical variables. The resulting p-values were corrected for multiple comparisons using the Benjamini–Hochberg FDR procedure, with significance set at an adjusted p-value < 0.05.

Following null findings from the primary analysis, we conducted exploratory post-hoc pairwise comparisons: the left vs. right-sided, the left vs. bilateral, the right vs. bilateral, and the unilateral vs. bilateral tinnitus comparison. For each comparison, we performed Wilcoxon rank-sum tests with FDR correction, effect size calculation using Cohen's d with 95% bootstrap confidence intervals, and ANCOVA with left-ear PTA (PTA_L) as a covariate to control for hearing thresholds. As a sensitivity analysis, we repeated the permutation ANCOVAs using either interaural PTA asymmetry (PTA_L–PTA_R) or mean PTA $[(PTA_L + PTA_R)/2]$ as the covariate. For each EEG feature, we summarized the laterality term's FDR-adjusted q-value and the covariate's partial η^2 . Post-hoc power analysis was conducted using G*Power 3.1 to determine the study's ability to detect effects of various magnitudes. All analyses were performed using R version 4.3.0. Statistical significance was set at $p < 0.05$ for exploratory (uncorrected) analyses, with FDR-adjusted $p < 0.05$ required for corrected significance.

Machine learning analysis

After the initial four-class model failed to meet the predetermined performance thresholds, we re-framed the task as a series of binary classifications encompassing every post-hoc pairwise comparison. Missing data were removed (complete-case analysis), and all predictors were z-standardized within resampling folds to prevent data leakage. Three algorithms were benchmarked: (i) RF with grid-tuned mtry; (ii) radial-basis-function SVM with cost and γ optimization; and (iii) Logistic Regression with L2 (ridge) regularization to mitigate overfitting in high-dimensional feature spaces. Hyperparameters were selected by an inner grid search nested within the outer resampling procedure. For validation, leave-one-out cross-validation was used when the smaller of the two classes contained fewer than 30 observations; otherwise, stratified five-fold cross-validation was applied. The nested design ensured that hyperparameter tuning relied solely on training data, yielding unbiased performance estimates. Synthetic minority over-sampling was applied within each training fold for binary tasks.

Primary endpoints were overall accuracy and balanced accuracy, each reported with 95% Wilson confidence intervals. Secondary metrics included sensitivity, specificity, AUC, and Cohen's κ . For the RF models, Gini-based feature importance scores were extracted and ranked to facilitate the biological interpretation of the most discriminative variables.

Data availability

The datasets used and/or analyzed during the current study available from the corresponding author on reasonable request.

Received: 21 May 2025; Accepted: 10 September 2025

Published online: 14 October 2025

References

1. Jarach, C. M. et al. Global Prevalence and Incidence of Tinnitus: A Systematic Review and Meta-analysis. *JAMA Neurol.* **79**, 888–900 (2022).
2. Lee, H. Y. & Jung, D. J. Recent Updates on Tinnitus Management. *J. Audiol. Otol.* **27**, 181–192 (2023).
3. Shore, S. E., Roberts, L. E. & Langguth, B. Maladaptive plasticity in tinnitus—triggers, mechanisms and treatment. *Nat. Rev. Neurol.* **12**, 150–160 (2016).
4. Shin, S. H., Byun, S. W., Lee, Z. Y., Park, Y. & Lee, H. Y. Clinical Features of Non-Lateralized Tinnitus. *J. Int. Adv. Otol.* **19**, 497–502X (2023).
5. Roberts, L. E., Husain, F. T. & Eggermont, J. J. Role of attention in the generation and modulation of tinnitus. *Neurosci. Biobehav. Rev.* **37**, 1754–1773 (2013).
6. Weisz, N., Moratti, S., Meinzer, M., Dohrmann, K. & Elbert, T. Tinnitus perception and distress is related to abnormal spontaneous brain activity as measured by magnetoencephalography. *PLoS Med.* **2**, e153 (2005).
7. Schlee, W. et al. Reduced variability of auditory alpha activity in chronic tinnitus. *Neural Plast.* **2014**, 436146 (2014).
8. van der Loo, E. et al. Tinnitus intensity dependent gamma oscillations of the contralateral auditory cortex. *PLoS ONE* **4**, e7396 (2009).
9. De Ridder, D., Vanneste, S., Song, J. J. & Adhia, D. Tinnitus and the Triple Network Model: A Perspective. *Clin. Exp. Otorhinolaryngol.* **15**, 205–212 (2022).
10. Kang, D. W., Kim, S. S., Park, D. C., Kim, S. H. & Yeo, S. G. Objective and Measurable Biomarkers in Chronic Subjective Tinnitus. *Int. J. Mol. Sci.* **22**, 6619 (2021).
11. Li, Z. et al. Objective Recognition of Tinnitus Location Using Electroencephalography Connectivity Features. *Front. Neurosci.* **15**, 784721 (2022).
12. Langguth, B., Kreuzer, P. M., Kleinjung, T. & De Ridder, D. Tinnitus: causes and clinical management. *Lancet Neurol.* **12**, 920–930 (2013).
13. De Ridder, D., Vanneste, S., Langguth, B. & Llinas, R. Thalamocortical Dysrhythmia: A Theoretical Update in Tinnitus. *Front. Neurol.* **6**, 124 (2015).
14. De Ridder, D. et al. Tinnitus and tinnitus disorder: Theoretical and operational definitions (an international multidisciplinary proposal). *Prog. Brain Res.* **260**, 1–25 (2021).
15. Shin, Y., Ryu, C.-W., Jahng, G.-H., Park, M. S. & Byun, J. Y. Changes in the laterality of functional connectivity associated with tinnitus: resting-state fMRI study. *Investig. Magn. Reson. Imaging* **23**, 55–64 (2019).
16. Song, J. J. et al. A quantitative electroencephalography study on cochlear implant-induced cortical changes in single-sided deafness with tinnitus. *Front. Hum. Neurosci.* **11**, 210 (2017).
17. Raeisi, Z. et al. Enhanced classification of tinnitus patients using EEG microstates and deep learning techniques. *Sci. Rep.* **15**(1), 15959 (2025).
18. Lee, H. Y., Shin, S. H. & Byun, S. W. Impact of short-term tinnitus treatment on cognitive function and neural synchronization. *Front. Neurol.* **16**, 1478033 (2025).

Acknowledgements

This research was supported by the National Research Foundation of Korea (NRF) grant funded by the Korea government (MSIT) (RS-2024-00352526).

Author contributions

S.J.K. conducted EEG data preprocessing and statistical analysis, and drafted the manuscript. S.H.S. contributed to data collection, clinical evaluation, and manuscript review. S.W.B. provided resources, supervised data validation, and critically revised the manuscript. H.Y.L. conceptualized the study, acquired funding, supervised the project, and edited the final manuscript. All authors reviewed and approved the final version of the manuscript.

Declarations

Competing interests

The authors declare no competing interests.

Additional information

Correspondence and requests for materials should be addressed to H.Y.L.

Reprints and permissions information is available at www.nature.com/reprints.

Publisher's note Springer Nature remains neutral with regard to jurisdictional claims in published maps and institutional affiliations.

Open Access This article is licensed under a Creative Commons Attribution-NonCommercial-NoDerivatives 4.0 International License, which permits any non-commercial use, sharing, distribution and reproduction in any medium or format, as long as you give appropriate credit to the original author(s) and the source, provide a link to the Creative Commons licence, and indicate if you modified the licensed material. You do not have permission under this licence to share adapted material derived from this article or parts of it. The images or other third party material in this article are included in the article's Creative Commons licence, unless indicated otherwise in a credit line to the material. If material is not included in the article's Creative Commons licence and your intended use is not permitted by statutory regulation or exceeds the permitted use, you will need to obtain permission directly from the copyright holder. To view a copy of this licence, visit <http://creativecommons.org/licenses/by-nc-nd/4.0/>.

© The Author(s) 2025